

## Three Iterative Finite Element Methods for the Stationary Smagorinsky Model

Haiyan Su<sup>1</sup>, Pengzhan Huang<sup>1</sup>, Juan Wen<sup>2</sup> and Xinlong Feng<sup>1,\*</sup>

<sup>1</sup> College of Mathematics and System Sciences, Xinjiang University, Urumqi 830046, P.R. China.

<sup>2</sup> Faculty of Science, Xi'an Jiaotong University, Xi'an 710049, P.R. China.

Received 23 September 2013; Accepted (in revised version) 12 March 2014.

Available online 7 April 2014

---

**Abstract.** Three iterative stabilised finite element methods based on local Gauss integration are proposed in order to solve the steady two-dimensional Smagorinsky model numerically. The Stokes iterative scheme, the Newton iterative scheme and the Oseen iterative scheme are adopted successively to deal with the nonlinear terms involved. Numerical experiments are carried out to demonstrate their effectiveness. Furthermore, the effect of the parameters  $Re$  (the Reynolds number) and  $\delta$  (the spatial filter radius) on the performance of the iterative numerical results is discussed.

**AMS subject classifications:** 65N30, 65N12, 76D07

**Key words:** Smagorinsky model, stabilised finite element method, local Gauss integration, iterative scheme, lid driven cavity flow.

---

### 1. Introduction

Large eddy simulation (*LES*) has attracted much attention over the last two decades, especially because increased computational resources have extended the range of scales that *LES* models might simulate. The *LES* approach is based upon a simple computational idea — i.e. approximate only the large structures in the flow, while modelling the influence of smaller ones. The large structures are defined by convolving the flow variables with a spatial filter of radius  $\delta$ . To model the effect of the discarded small structures, traditionally physical insight from the statistical theory of turbulence (such as the energy cascade) has been used. The Smagorinsky model is one of the most popular *LES* models, where this physically-based approach involves introducing an artificial viscosity term that dissipates energy in the large scale structure at the same rate as the discarded small structures would have dissipated had they been included in the model.

---

\*Corresponding author. Email addresses: yanzi880308xju@sina.com (H. Su), hpzh007@gmail.com (P. Huang), zhongnanjicuan@163.com (J. Wen), fxlmath@gmail.com (X. Feng)

In this article, we consider the following steady Smagorinsky model:

$$-\nu \Delta u - \nabla \cdot ((C_S \delta)^2 |\nabla u| \nabla u) + (u \cdot \nabla) u + \nabla p = f \quad \text{in } \Omega, \quad (1.1)$$

$$\nabla \cdot u = 0 \quad \text{in } \Omega, \quad (1.2)$$

$$u = 0 \quad \text{on } \partial\Omega. \quad (1.3)$$

Here  $\Omega$  is a bounded, convex and open subset of  $\mathbb{R}^2$  with a Lipschitz-continuous boundary  $\partial\Omega$ ,  $u$  represents the velocity vector,  $p$  the pressure,  $f$  the prescribed spatially filtered forcing term,  $C_S$  the Smagorinsky constant,  $\delta$  the radius of the spatial filter used in the *LES* model,  $\nu > 0$  the viscosity inversely proportional to the Reynolds number  $Re$ , and  $|\sigma| = \sqrt{\sum_{i,j=1}^2 |\sigma_{ij}|^2}$  the Frobenius norm of the tensor  $\sigma$ .

There are numerous works devoted to the development of efficient schemes for solving the stationary Smagorinsky model [5–8, 13]. It is well known that numerical computations for the stationary Smagorinsky model can be performed by iterative procedures, and in practice one usually takes the solution of the Stokes equations as the initial iterative input. The stationary Smagorinsky equations are then solved by an iterative procedure until the norm of the difference in successive iterations falls within a fixed tolerance. Usually, efficient approximations of the transient Smagorinsky equations are based on a semi-discretisation in time, followed by a spatial discretisation at each time step — e.g. using finite elements to solve the stationary Smagorinsky equations at each time step. However, a search for the most efficient numerical methods to solve the stationary Smagorinsky model is justified.

Finite element methods (FEMs) are widely used in computational fluid dynamics. In particular, some stable mixed FEMs are often a basic component in efficiently solving the incompressible flow equations. Of the mixed element methods, equal-order velocity-pressure pairs have proven quite practical in finite element approximations of the Smagorinsky problem, but they violate the inf-sup condition [14] and the compatibility between the velocity and pressure spaces. In using a primitive variable formulation, the importance of ensuring the compatibility of the component approximations of velocity and pressure by satisfying the so-called inf-sup condition is therefore widely understood. This condition has played an important role because it ensures a stability and accuracy of the underlying numerical schemes — thus a pair of finite element spaces to approximate the velocity and pressure unknowns are said to be stable if they satisfy the inf-sup condition. Intuitively, this condition enforces a certain correlation between the two finite element spaces, so that they both have the required properties when employed for the Navier-Stokes equations.

However, due to computational convenience and efficiency in practice, some mixed finite element pairs that do not satisfy the inf-sup condition are also popular. Consequently, considerable attention has been paid to the study of stabilised methods for the Stokes and Navier-Stokes problems. Recent studies have focused on stabilisation of the lowest equal-order finite element pair (piecewise linear polynomials) using the projection of the pressure onto the piecewise constant space [2, 4, 5, 9, 10, 12], a technique that does not require specification of stabilising parameters or edge-based data structure. There are some important advantages over traditionally stabilised mixed finite element methods —

notably simplicity, efficiency and independence of the stabilisation parameters — so this approach is gaining increasing popularity in computational fluid dynamics.

Here we combine the lowest equal-order stabilised finite element method with Stokes, Newton and Oseen iterative schemes based on the Gaussian quadrature rule, involving two steps — viz. we solve a Stokes problem to give the initial values, and then the Smagorinsky model by each of the three iterative methods. Moreover, we investigate the effect of the parameters  $Re$  and  $\delta$  on the performance of the numerical results. The rest of this article is organised as follows. After introducing some notation, in the next section we discuss relevant functional spaces and a variable formulation of the Smagorinsky equations. The corresponding mixed finite element spaces and stabilised discrete weak formulation are presented in Section 3, and the three iterative stabilised FEMs proposed for the Smagorinsky model are detailed in Section 4. In Section 5, numerical experiments are given to illustrate existing theoretical results, and our concluding remarks follow in Section 6.

## 2. Preliminaries

As mentioned, after introducing the necessary function spaces we present an appropriate mathematical setting to facilitate approximate solutions for the Smagorinsky model. Thus for  $\Omega \subset \mathbb{R}^2$ , let  $L^r(\Omega)$ ,  $W_0^{k,r}(\Omega)$ ,  $k = 0, 1, \dots$ , denote the usual Sobolev spaces [1]. Let  $\|\cdot\|$  denote the norm on  $L^2(\Omega)$ ,  $\|\cdot\|_r = \|\cdot\|_{0,r}$  the norm on  $L^r(\Omega)$ ,  $\|\cdot\|_{k,r}$  the norm on  $W^{k,r}(\Omega)$ , and  $(\cdot, \cdot)$  denote the scalar product in  $L^2(\Omega)$ . We then introduce the Hilbert spaces

$$X = (W_0^{1,3}(\Omega))^2, \quad M = L_0^2(\Omega) = \{q \in L^2(\Omega) : \int_{\Omega} q dx = 0\},$$

and define two continuous bilinear forms  $a(\cdot, \cdot)$ ,  $d(\cdot, \cdot)$  and a generalised bilinear form  $B((\cdot, \cdot); (\cdot, \cdot))$  on  $(X, X)$ ,  $(X, M)$  and  $(X, M) \times (X, M)$  respectively as

$$a(u, v) = \nu(\nabla u, \nabla v), \quad \forall u, v \in X, \quad d(v, q) = (q, \operatorname{div} v), \quad \forall v \in X, \quad \forall q \in M,$$

and

$$B((u, p); (v, q)) = a(u, v) - d(v, p) + d(u, q), \quad \forall (u, p), (v, q) \in (X, M),$$

and a trilinear form on  $(X, X, X)$  by

$$a_1(u, v, w) = ((u \cdot \nabla)v, w), \quad \forall u, v, w \in X.$$

In order to solve the problem (1.1)–(1.3) numerically, we also introduce the trilinear form

$$b(u; v, w) = \left( (u \cdot \nabla)v + \frac{1}{2} \operatorname{div} uv, w \right) = \frac{1}{2} a_1(u, v, w) - \frac{1}{2} a_1(u, w, v)$$

$\forall u, v, w \in X$ , and write

$$a_0(u, v, w) = (C_S \delta)^2 (|\nabla u| \nabla v, \nabla w), \quad \forall u, v, w \in X.$$

With the above notation, the formulation of the problem (1.1)–(1.3) reads as follows: find  $(u, p) \in (X, M)$  such that for all  $(v, q) \in (X, M)$

$$B((u, p); (v, q)) + a_0(u, u, v) + b(u; u, v) = (f, v). \quad (2.1)$$

We know that there exists at least a solution which satisfies (2.1) and the solution is unique [7]. Furthermore, we have

$$\|u\|_{1,3} \leq (C_S \delta)^{-1} \|f\|_{-1,3}^{1/2}, \quad \|f\|_{-1,3} = \sup_{v \in X} \frac{|(f, v)|}{\|\nabla v\|_{1,3}},$$

and

$$\|\nabla u\|_0 \leq \Psi(\|f\|_{-1}), \quad \|f\|_{-1} = \sup_{v \in H_0^1(\Omega)} \frac{|(f, v)|}{\|\nabla v\|_0}.$$

### 3. Mixed Finite Element Spaces

Let  $h > 0$  be a real positive parameter and  $T_h = \bigcup_{j=1}^J K_j$  be the regular triangulation of the domain  $\Omega$  with the mesh parameter  $h = \max\{\text{diam}(K_j)\}$ . The finite element subspace  $(X_h, M_h)$  of  $(X, M)$  characterised by  $T_h$  is assumed to be uniformly regular as  $h \rightarrow 0$ , and we can establish the conforming velocity-pressure finite element space pair  $(X_h, M_h) \subset (X, M)$  based on  $T_h$ . We define

$$\begin{aligned} X_h &= \{u \in C^0(\overline{\Omega})^2 \cap X : u|_K \in P_1(K)^2, \quad \forall K \in T_h(\Omega)\}, \\ M_h &= \{q \in C^0(\overline{\Omega}) \cap M : q|_K \in P_1(K), \quad \forall K \in T_h(\Omega)\}, \end{aligned}$$

where  $P_1(K)$  represents the space of linear polynomials on the set  $K$ . Next, we introduce the standard discretisation of the problem (2.1) to find  $(u_h, p_h) \in (X_h, M_h)$  such that

$$B((u_h, p_h); (v, q)) + a_0(u_h, u_h, v) + b(u_h; u_h, v) = (f, v), \quad \forall (v, q) \in (X_h, M_h),$$

where

$$B((u_h, p_h); (v, q)) = a(u_h, v) - d(v, p_h) + d(u_h, q).$$

It is notable that the equal-order velocity-pressure pair  $(X_h, M_h)$  does not satisfy the discrete inf-sup condition, and in order to fulfil this condition a stabilised generalised bilinear term is used [9]:

$$B_h((u_h, p_h); (v, q)) + a_0(u_h, u_h, v) + b(u_h; u_h, v) = (f, v), \quad \forall (v, q) \in (X_h, M_h), \quad (3.1)$$

where  $G_h(p_h, q)$  can be defined by

$$G(p_h, q) = \sum_{K_j \in T_h} \left\{ \int_{K_{j,2}} p_h q dx - \int_{K_{j,1}} p_h q dx \right\}, \quad p, q \in L^2(\Omega),$$

with  $\int_{K_{j,i}} pq dx$  an appropriate Gauss integral over  $K_j$  that is exact for a polynomial of degree  $i$  ( $i = 1, 2$ ) and  $p_h q$  is a polynomial of degree not greater than 2. Thus the stabilising term  $G(\cdot, \cdot)$  defined by the difference of Gauss quadratures must be exact for all test functions  $q \in M_h$ , and the trial function  $p_h \in P_0$  (piecewise constant) when  $i = 1$ .

Consequently, we define the  $L^2$ -projection operator  $\pi_h: L^2(\Omega) \rightarrow W_h$  by

$$(p, q_h) = (\pi_h p, q_h), \quad \forall p \in L^2(\Omega), \quad q_h \in W_h,$$

where  $W_h \subset L^2(\Omega)$  denotes the piecewise constant space associated with  $T_h$ . Further, we define the stability term as

$$G(p, q) = (p - \pi_h p, q - \pi_h q). \quad (3.2)$$

Finally, the stabilised discrete weak formulation of the Smagorinsky model is to find  $(u_h, p_h) \in (X_h, M_h)$  such that

$$B_h((u_h, p_h); (v, q)) + a_0(u_h, u_h, v) + b(u_h; u_h, v) = (f, v), \quad \forall (v, q) \in (X_h, M_h), \quad (3.3)$$

where the bilinear term

$$B_h((u_h, p_h); (v, q)) = B((u_h, p_h); (v, q)) + G(p_h, q).$$

Given earlier results on the stabilised method [10] and on applying a similar method as in Ref. [7], we have the stability and error estimates as follows.

**Theorem 3.1.** *Let  $(u, p) \in ((H^2(\Omega)^2 \cap X), H(\Omega) \cap M)$ . Then  $u_h$  defined by the scheme (3.3) satisfies*

$$\|\nabla u_h\|_0 \leq \Psi(\|f\|_{-1}), \quad (3.4)$$

$$\|u_h\|_{1,3} \leq (c_0(C_S \delta)^{-2} \|f\|_{-1})^{1/2}, \quad (3.5)$$

and the bounds

$$\|\nabla(u - u_h)\|_0 \leq ch(1 + \delta^2)(\|u\|_2 + \|p\|_1), \quad (3.6)$$

$$\|u - u_h\|_{1,3} \leq ch^{2/3}(1 + \delta^2)(\|u\|_{2,3} + \|p\|_{1,3}). \quad (3.7)$$

#### 4. Three Iterative Stabilised FEMs

Let us now focus on numerically comparing the three iterative stabilised FEMs for solving the stationary Smagorinsky model to obtain  $(u_h^n, p_h^n) \in (X_h, M_h)$  as listed below [3].

**Algorithm I (Stokes iterative scheme):**

$$B_h((u_h^n, p_h^n); (v, q)) = (f, v) - b(u_h^{n-1}; u_h^{n-1}, v) - a_0(u_h^{n-1}, u_h^{n-1}, v), \quad (4.1)$$

**Algorithm II (Newton iterative scheme):**

$$\begin{aligned}
& B_h \left( (u_h^n, p_h^n); (v, q) \right) + b(u_h^n; u_h^{n-1}, v) + b(u_h^{n-1}; u_h^n, v) \\
& + a_0(u_h^{n-1}, u_h^n, v) + (C_S \delta)^2 \left( \frac{[\nabla u_h^{n-1} : \nabla u_h^n]}{\nabla u_h^{n-1}} \nabla u_h^{n-1}, \nabla v \right) \\
& = b(u_h^{n-1}; u_h^{n-1}, v) + a_0(u_h^{n-1}, u_h^{n-1}, v) + (f, v),
\end{aligned} \tag{4.2}$$

where  $\nabla v : \nabla w = \sum_{i,j}^2 \frac{\partial v_i}{\partial x_j} \frac{\partial w_i}{\partial x_j}$ .

**Algorithm III (the Oseen iterative scheme):**

$$B_h \left( (u_h^n, p_h^n); (v, q) \right) + b(u_h^{n-1}; u_h^n, v) + a_0(u_h^{n-1}, u_h^n, v) = (f, v), \tag{4.3}$$

for all  $(v, q) \in (X_h, M_h)$ .

As indicated previously, in each algorithm  $(u_h^0, p_h^0) \in (X_h, M_h)$  is defined by the discrete Stokes problem:

$$a(u_h^0, v) - d(v, p_h^0) + d(u_h^0, q) = (f, v), \tag{4.4}$$

for all  $(v, q) \in (X_h, M_h)$ .

Let us now discuss the two-dimensional implementation of these three iterative stabilised FEMs, where we use the conforming  $(P_1, P_1)$  spaces  $(X_h, M_h)$ . We write the velocity and pressure vector

$$u_h = \begin{pmatrix} u_{h1} \\ u_{h2} \end{pmatrix}, \quad p_h = (p_h),$$

and the test function vector

$$v = \begin{pmatrix} v_1 \\ v_2 \end{pmatrix}, \quad q = (q),$$

and suppose the spaces  $X_h$  and  $M_h$  are equipped with the bases

$$X_h = \text{span}\{\varphi_i : i = 1, \dots, \mathcal{N}\}, \quad M_h = \text{span}\{\psi_i : i = 1, \dots, \mathcal{M}\},$$

where  $N$  and  $M$  indicate the number in each of the bases of  $X_h$  and  $M_h$ , respectively. Then

$$\begin{aligned}
u_h &= \sum_{i=1}^{\mathcal{N}} u_{hi} \varphi_i, \quad v = \varphi_j, \quad j = 1, \dots, \mathcal{N}, \\
p_h &= \sum_{i=1}^{\mathcal{M}} p_i \psi_i, \quad q = \psi_j, \quad j = 1, \dots, \mathcal{M}.
\end{aligned}$$

After linearisation in the Stokes, Newton or Oseen iterations, we obtain a linear saddle point problem of the form

$$\begin{pmatrix} \mathcal{A} & \mathcal{B} \\ \mathcal{C} & \mathcal{D} \end{pmatrix} \begin{pmatrix} U_h^n \\ P_h^n \end{pmatrix} = \begin{pmatrix} F \\ 0 \end{pmatrix},$$

where  $U_h^n = (u_{h1}^n, u_{h2}^n, \dots, u_{h\mathcal{N}}^n)^T$ ,  $P_h^n = (p_{h1}^n, p_{h2}^n, \dots, p_{h\mathcal{M}}^n)^T$  and  $F$  is the known term for the iterative stabilised FEMs.

- For Algorithm I, straightforward calculation gives

$$\begin{aligned} (\mathcal{A})_{i,j} &= a(\varphi_i, \varphi_j), \quad i, j = 1, \dots, \mathcal{N}, \\ (\mathcal{B})_{i,j} &= -d(\varphi_j, \psi_i), \quad i = 1, \dots, \mathcal{M}, \quad j = 1, \dots, \mathcal{N}, \\ (\mathcal{C})_{i,j} &= -d(\varphi_i, \psi_j), \quad i = 1, \dots, \mathcal{N}, \quad j = 1, \dots, \mathcal{M}, \\ (\mathcal{D})_{i,j} &= -G(\psi_i, \psi_j), \quad i, j = 1, \dots, \mathcal{M}. \end{aligned}$$

It is well known that  $a(\cdot, \cdot)$  and  $G(\cdot, \cdot)$  are symmetrical, and  $(\mathcal{B})_{i,j} = (\mathcal{C})_{j,i}$ , producing a symmetric iterative matrix for Algorithm I.

- However, for Algorithm II

$$\begin{aligned} (\mathcal{A})_{i,j} &= a(\varphi_i, \varphi_j) + b(\varphi_i; u_h^{n-1}, \varphi_j) + b(u_h^{n-1}; \varphi_i, \varphi_j) + a_0(u_h^{n-1}, \varphi_i, \varphi_j) \\ &\quad + (C_S \delta)^2 \left( \frac{[\nabla u_h^{n-1} : \nabla \varphi_i]}{\nabla u_h^{n-1}} \nabla u_h^{n-1}, \nabla \varphi_j \right), \quad i, j = 1, \dots, \mathcal{N}, \\ (\mathcal{B})_{i,j} &= -d(\varphi_j, \psi_i), \quad i = 1, \dots, \mathcal{M}, \quad j = 1, \dots, \mathcal{N}, \\ (\mathcal{C})_{i,j} &= -d(\varphi_i, \psi_j), \quad i = 1, \dots, \mathcal{N}, \quad j = 1, \dots, \mathcal{M}, \\ (\mathcal{D})_{i,j} &= -G(\psi_i, \psi_j), \quad i, j = 1, \dots, \mathcal{M}, \end{aligned}$$

and  $(\mathcal{A})_{i,j} \neq (\mathcal{A})_{j,i}$  so the iterative matrix is asymmetric.

- In the case of Algorithm III, we have

$$\begin{aligned} (\mathcal{A})_{i,j} &= a(\varphi_i, \varphi_j) + b(u_h^{n-1}; \varphi_i, \varphi_j) + a_0(u_h^{n-1}, \varphi_i, \varphi_j), \quad i, j = 1, \dots, \mathcal{N}, \\ (\mathcal{B})_{i,j} &= -d(\varphi_j, \psi_i), \quad i = 1, \dots, \mathcal{M}, \quad j = 1, \dots, \mathcal{N}, \\ (\mathcal{C})_{i,j} &= -d(\varphi_i, \psi_j), \quad i = 1, \dots, \mathcal{N}, \quad j = 1, \dots, \mathcal{M}, \\ (\mathcal{D})_{i,j} &= -G(\psi_i, \psi_j), \quad i, j = 1, \dots, \mathcal{M}, \end{aligned}$$

so due to the asymmetry of matrix  $\mathcal{A}$  (i.e.  $(\mathcal{A})_{i,j} \neq (\mathcal{A})_{j,i}$ ) the iterative matrix is again asymmetric.

Algorithm I is completely linearised (previously  $a_0(u_h, u_h, v)$  and  $b(u_h; u_h, v)$  nonlinear) but implicit in the linear term  $B_h((u_h, p_h); (v, q))$ , so the resulting iterative matrix is invariant such that a classical iterative method can be used. However, in Algorithms II and III the standard Newton and Oseen iterations are respectively applied in respect of both nonlinear terms, so implicit forms are obtained, and the generalised minimal residual (GMRES) method can be used to deal with their variable iterative matrices.

## 5. Numerical Experiments

We first consider the performance of the several kinds of algorithm described in this article, and then present the results of our tests for the three iterative stabilised FEMs for the discretisation of the Smagorinsky model. Our computational experiments emphasise three main areas of interest associated with the three iterative stabilised FEM simulations — viz. (1) verifying optimal finite element convergence estimates; (2) investigating relative errors in the velocity under the norms  $L^2$  and  $H^1$  and the pressure under the norm  $L^2$  for various values of the parameters  $Re$  and  $\delta$ ; and (3) comparing the number of the iterations for various values of the parameters  $Re$  and  $\delta$ .

The performance was explored using an analytical problem. In the computations, the pressure and velocity are approximated by the lowest equal-order finite element pair defined with respect to a unit-square domain in  $\mathbb{R}^2$ , using the same uniform triangulation of  $\Omega$  into triangles. The Smagorinsky constant adopted was  $C_S = 0.17$ , which is a popular choice in practical turbulence computations. The  $H^1$ -norm and  $L^2$ -norm of the relative error for the velocity and  $L^2$ -norm of the relative error for the pressure are presented in the

Table 1: A comparison of the  $H^1$ -relative-error,  $L^2$ -relative-error for  $u$  and  $L^2$ -relative-error for  $p$ , and the number of iterative steps, for Algorithm 1 with various values of  $Re$ ,  $H$  and  $\delta$ .

$1/H$	$Re$	$\delta$	$uL^2 - error$	$uH^1 - error$	$pL^2 - error$	iter.no.
45	1	31.6	N/A	N/A	N/A	diverges
45	1	3.16	0.019177	0.071528	0.006054	4
45	1	0.316	0.014599	0.070876	0.006015	2
45	1	0.0316	0.014575	0.070876	0.006015	2
63	1	31.6	N/A	N/A	N/A	diverges
63	1	3.16	0.013417	0.049623	0.003417	4
63	1	0.316	0.007504	0.048641	0.003394	2
63	1	0.0316	0.007479	0.048641	0.003394	2
45	100	31.6	N/A	N/A	N/A	diverges
45	100	3.16	N/A	N/A	N/A	diverges
45	100	0.316	0.020410	0.116583	0.001564	5
45	100	0.0316	0.015916	0.116449	0.001562	5
63	100	31.6	N/A	N/A	N/A	diverges
63	100	3.16	N/A	N/A	N/A	diverges
63	100	0.316	0.013813	0.073265	0.000869	5
63	100	0.0316	0.007972	0.072731	0.000867	5
45	1000	31.6	N/A	N/A	N/A	diverges
45	1000	3.16	N/A	N/A	N/A	diverges
45	1000	0.316	N/A	N/A	N/A	diverges
45	1000	0.0316	N/A	N/A	N/A	diverges
63	1000	31.6	N/A	N/A	N/A	diverges
63	1000	3.16	N/A	N/A	N/A	diverges
63	1000	0.316	N/A	N/A	N/A	diverges
63	1000	0.0316	N/A	N/A	N/A	diverges



Table 2: A comparison of the  $H^1$ -relative-error,  $L^2$ -relative-error for  $u$  and  $L^2$ -relative-error for  $p$ , and the number of iterative steps, for Algorithm II with various values of  $Re$ ,  $H$  and  $\delta$ .

$1/H$	$Re$	$\delta$	$uL^2 - error$	$uH^1 - error$	$pL^2 - error$	iter.no.
45	1	31.16	N/A	N/A	N/A	diverges
45	1	3.16	0.122911	0.137893	0.006559	2
45	1	0.316	0.014950	0.070885	0.006020	1
45	1	0.0316	0.014578	0.070876	0.006015	1
63	1	31.6	N/A	N/A	N/A	diverges
63	1	3.16	0.120841	0.128149	0.003710	2
63	1	0.316	0.007906	0.048657	0.003397	1
63	1	0.0316	0.007482	0.048641	0.003394	1
45	100	31.6	N/A	N/A	N/A	diverges
45	100	3.16	N/A	N/A	N/A	diverges
45	100	0.316	0.123355	0.164194	0.001591	2
45	100	0.0316	0.016269	0.116429	0.001562	1
63	100	31.6	N/A	N/A	N/A	diverges
63	100	3.16	N/A	N/A	N/A	diverges
63	100	0.316	0.120974	0.138413	0.000885	2
63	100	0.0316	0.008378	0.07273	0.000867	1
45	1000	31.6	N/A	N/A	N/A	diverges
45	1000	3.16	N/A	N/A	N/A	diverges
45	1000	0.316	N/A	N/A	N/A	diverges
45	1000	0.0316	0.025729	0.174348	0.001292	2
63	1000	31.6	N/A	N/A	N/A	diverges
63	1000	3.16	N/A	N/A	N/A	diverges
63	1000	0.316	N/A	N/A	N/A	diverges
63	1000	0.0316	0.018252	0.113716	0.000674	2

Tables 1-3 and Table 4 for  $Re = 1, 100, 1000$ . with  $\delta$  values 31.6, 3.16, 0.316 and 0.0316. The nonlinear problem was solved using the stopping criterion  $10^{-6}$  for the maximum successive errors in both  $u$  and  $p$  in the  $L^2$  and  $H^1$  norm.

In the two-dimensional problem adopted, the function  $f(x, y)$  on the right-hand-side in the Smagorinsky equations (1.1)-(1.3) involved the following prescribed exact velocity  $u = (u_1, u_2)$  and pressure  $p$ :

$$\begin{aligned}
 u_1(x, y) &= 10x^2(x-1)^2y(y-1)(2y-1), \\
 u_2(x, y) &= -10x(2x-1)y^2(y-1)^2, \\
 p(x, y) &= 10(2x-1)(2y-1).
 \end{aligned}$$

### 5.1. Analysis of discretisation errors with various $Re$ , $H$ , and $\delta$ .

Let us first discuss the dependency of the magnitudes of the discretisation errors on the Reynolds number, the mesh-size, and filter radius. The results for the  $L^2$  and  $H^1$  relative norms for  $u$ , and the  $L^2$  relative norm for  $p$ , are presented in Tables 1 to 3 for the Stokes

Table 3: A comparison of the  $H^1$ -relative-error,  $L^2$ -relative-error for  $u$  and  $L^2$ -relative-error for  $p$ , and the number of iterative steps, for Algorithm III for various values of  $Re$ ,  $H$  and  $\delta$ .

$1/H$	$Re$	$\delta$	$uL^2 - error$	$uH^1 - error$	$pL^2 - error$	iter.no.
45	1	31.6	N/A	N/A	N/A	diverges
45	1	3.16	0.079281	0.103861	0.006258	5
45	1	0.316	0.014811	0.070880	0.006017	2
45	1	0.0316	0.014577	0.070876	0.006015	2
63	1	31.6	N/A	N/A	N/A	diverges
63	1	3.16	0.076852	0.090378	0.003564	5
63	1	0.316	0.007738	0.048649	0.003395	2
63	1	0.0316	0.007481	0.048641	0.003394	2
45	100	31.6	N/A	N/A	N/A	diverges
45	100	3.16	N/A	N/A	N/A	diverges
45	100	0.316	0.080039	0.137861	0.001576	5
45	100	0.0316	0.016130	0.116437	0.001562	3
63	100	31.6	N/A	N/A	N/A	diverges
63	100	3.16	N/A	N/A	N/A	diverges
63	100	0.316	0.077088	0.104860	0.000875	5
63	100	0.0316	0.008210	0.072728	0.000867	3
45	1000	31.6	N/A	N/A	N/A	diverges
45	1000	3.16	N/A	N/A	N/A	diverges
45	1000	0.316	0.345987	0.383074	0.001319	13
45	1000	0.0316	0.022624	0.174087	0.001292	6
63	1000	31.6	N/A	N/A	N/A	diverges
63	1000	3.16	N/A	N/A	N/A	diverges
63	1000	0.316	0.337613	0.355601	0.000713	13
63	1000	0.0316	0.014428	0.113315	0.000674	6

iterative scheme, Newton iterative scheme and Oseen iterative scheme respectively, and may be summarised as follows.

(i) The  $L^2$  relative error and  $H^1$  relative error of  $u$  and  $L^2$  relative error of  $p$  weakened when the value of  $\delta$  varied from 31.6 to 0.0316;

(ii) When the value of  $1/H$  varied from 45 to 63, the  $L^2$  relative error and  $H^1$  relative error of  $u$  and  $L^2$  relative error of  $p$  weakened;

(iii) When the value of  $Re$  varied from 1 to 1000, the  $L^2$  relative error and  $H^1$  relative error of  $u$  increased but the  $L^2$  relative error of  $p$  weakened.

## 5.2. Analysis of the influence of $Re$ , $\delta$ and $H$ on the number of iterations.

A close inspection of Tables 1 to 3 also identifies the dependency of the number of iterative steps on the parameters  $Re$  and  $\delta$  — viz.

(i) If  $\delta$  increases, the number of iterative steps grows;

(ii)  $H$  does not affect the number of iterative steps;

(iii) For larger  $Re$  have been chosen, the number of iterative steps is larger.

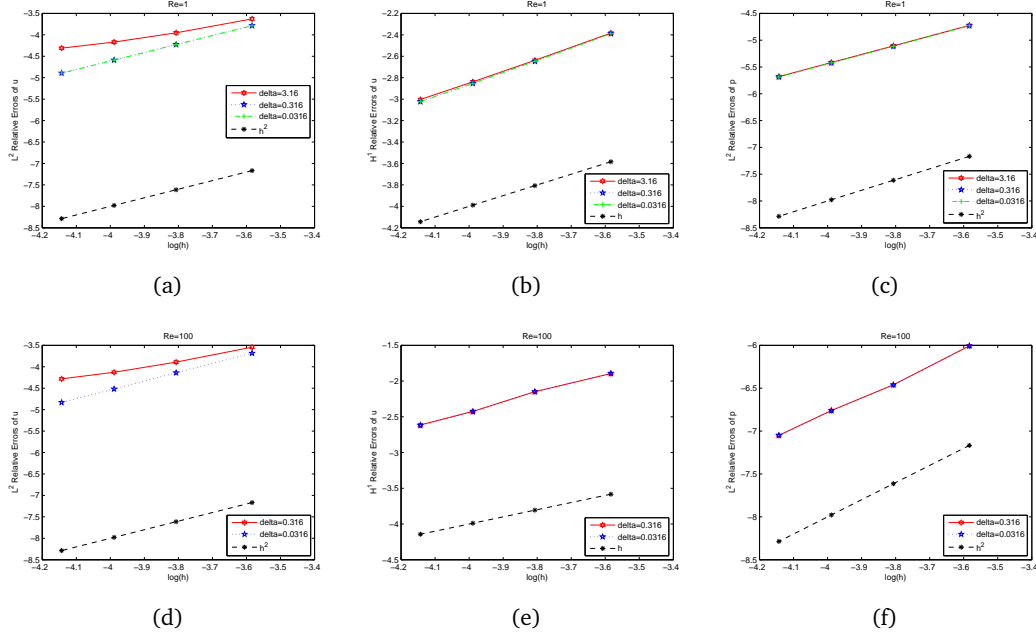


Figure 1: Rate analysis of Algorithm I with  $Re = 1, 100$  for various  $\delta$ . (a, d)  $L^2$ -error for the velocity; (b, e)  $H^1$ -error for the velocity; (c, f)  $L^2$ -error for the pressure.

### 5.3. Optimal rate analysis under various parameters $Re$ , $H$ , and $\delta$ .

From the point of view of precision, Figs. 1 to 3 show that the three iterative stabilised FEMs (with various parameters) all have good convergence order for smaller  $Re$  and lower  $\delta$ , but diverge for larger  $\delta$  and  $Re$ .

In general, the Stokes iteration scheme is restrictive in the choice of Reynolds number  $Re$  and filter radius  $\delta$ , the Newton iteration scheme less so, whereas the Oseen iterative scheme is far less so. The number of iterations is least for the Newton iteration scheme and greatest for the Stokes iteration scheme, while the relative errors are almost the same for all three schemes. It appears that the Newton scheme is the best for smaller  $Re$  and lower  $\delta$ , when it can reach an optimal convergence rate with the relatively small error in both  $u$  and  $p$  and with the fewest iterative steps. However, none of the three iterative stabilised FEMs appear suitable for numerically solving the Smagorinsky model at large Reynolds numbers and filter radii, which could be because the iterative matrices are then not diagonally dominant.

### 5.4. Numerical simulations of lid driven cavity flow.

We also tested a popular benchmark problem — viz. the lid-driven cavity, where the computation was carried out in the region  $\Omega = \{(x, y) | 0 < x, y < 1\}$ . Here we impose the condition that the normal component of the velocity is zero on its boundary  $\partial\Omega$ , and also that the tangential component of the velocity is zero except along  $y = 1$  where it is set

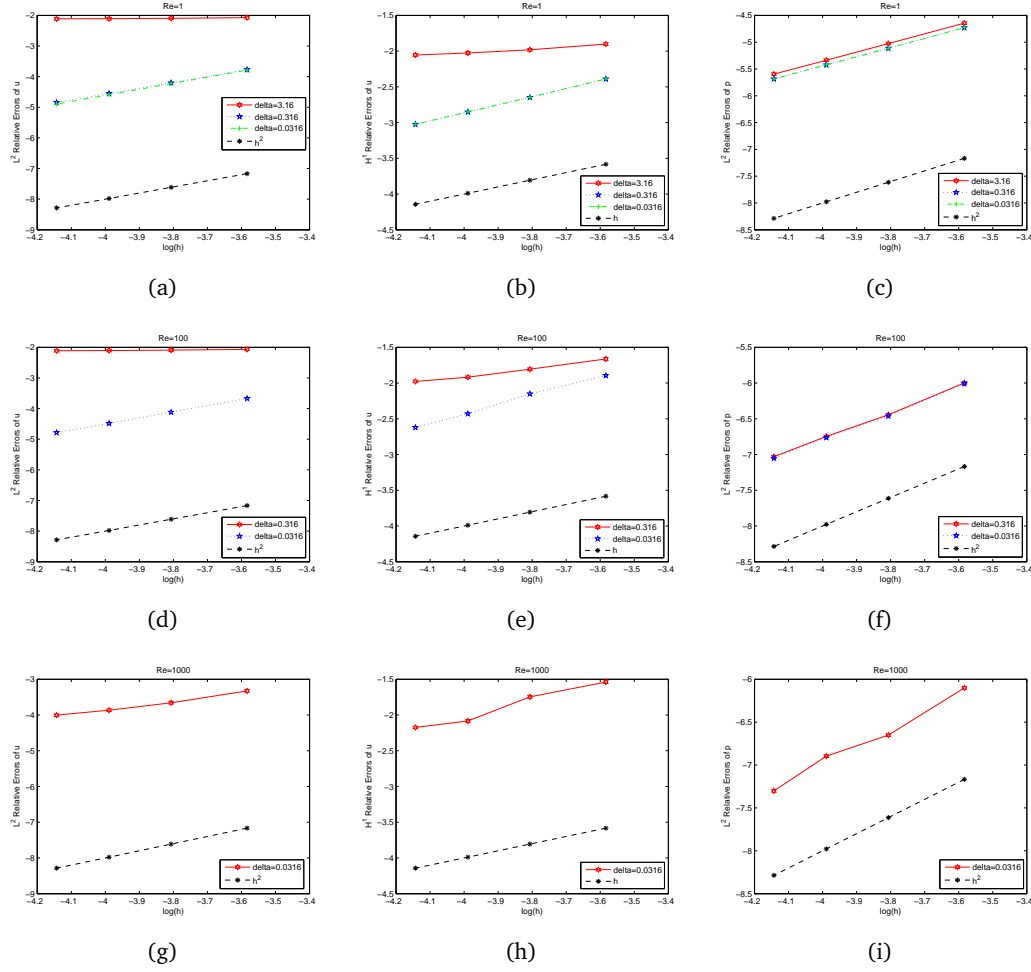


Figure 2: Rate analysis of Algorithm II with  $Re = 1, 100, 1000$  for various  $\delta$ . (a, d, g)  $L^2$ -error for the velocity; (b, e, h)  $H^1$ -error for the velocity; (c, f, i)  $L^2$ -error for the pressure.

to be 1. This problem was chosen because it offers a realistic flow setting where we can investigate whether the proposed algorithms are practical for the Smagorinsky model.

The results for the Algorithms I-III were computed on a fine mesh ( $h = 1/64$ ), for the Reynolds numbers  $Re = 1, 100$  and  $1000$  and spatial filter radii  $\delta = 3.16, 0.316$  and  $0.0316$ . Figs. 4-9 show the corresponding velocity streamlines and pressure contours for this cavity flow.

Algorithm I only worked for  $Re = 1$  with  $\delta = 0.0316$  modes; and Algorithm ran for  $Re = 1$  with  $\delta = 3.16, 0.316$  and  $0.0316$ , and  $Re = 100$  with  $\delta = 0.0316$ . On the other hand, Algorithm III dealt with all of the  $Re$  and  $\delta$  values chosen, except for  $Re = 100$  and  $1000$  with  $\delta = 31.6$ . This reinforces our view from the first example — viz. that the Oseen iterative scheme is best over a range of values of the Reynolds number  $Re$  and filter radius  $\delta$ , the Newton iteration scheme next best, and the Stokes iteration scheme is most

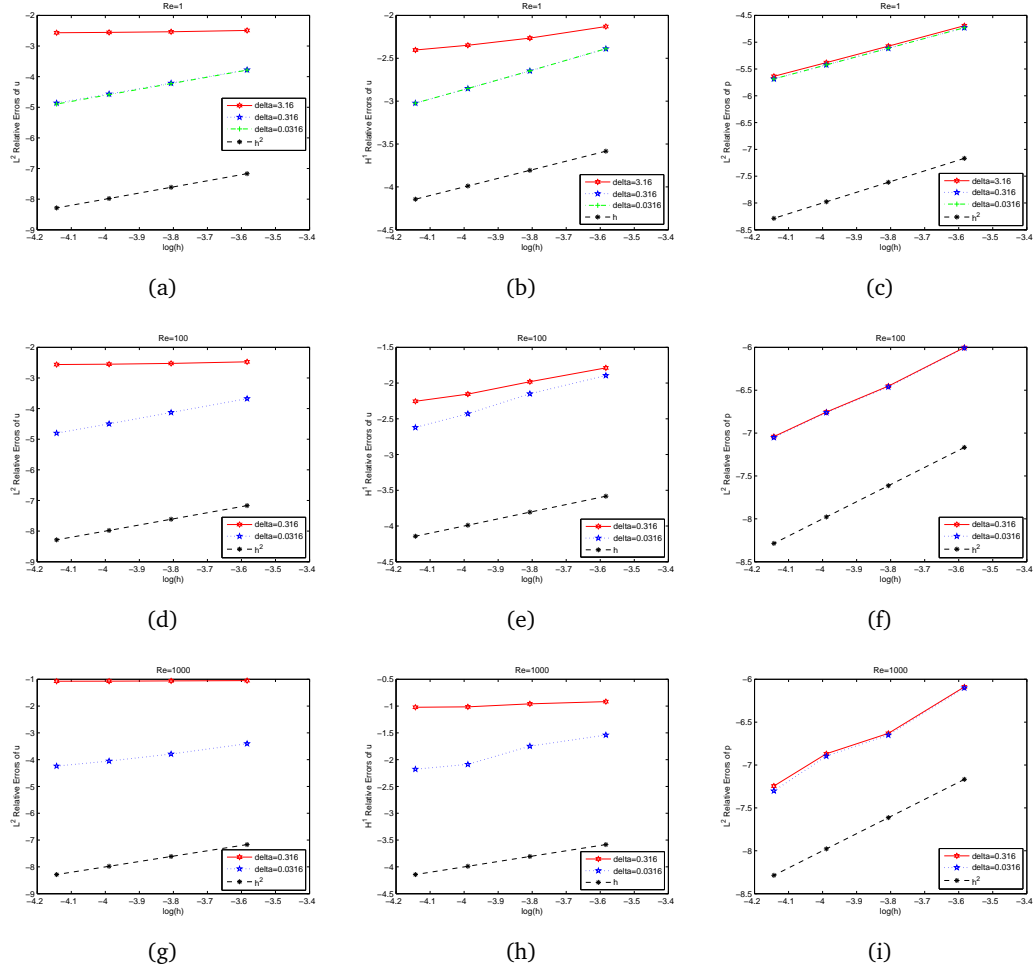


Figure 3: Rate analysis of Algorithm III with  $Re = 1, 100, 1000$  for various  $\delta$ . (a, d, g)  $L^2$ -error for the velocity; (b, e, h)  $H^1$ -error for the velocity; (c, f, i)  $L^2$ -error for the pressure.

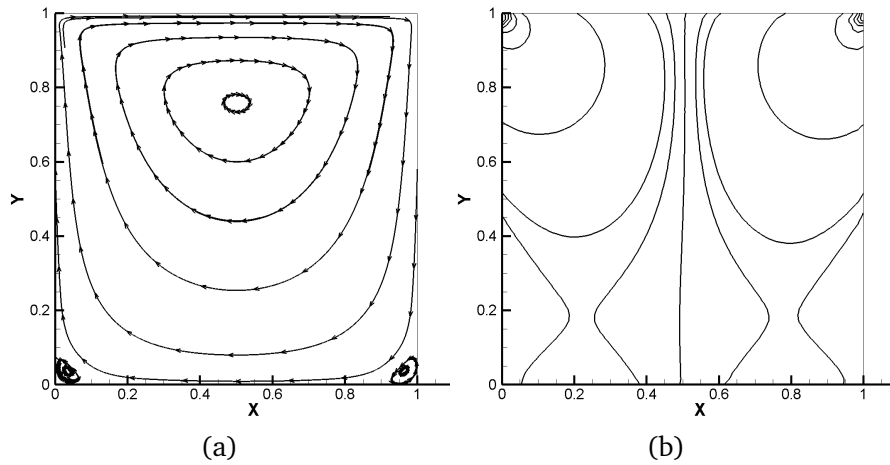


Figure 4: Velocity streamlines (a) and pressure level lines (b) by Algorithm I with  $\delta = 0.0316$  for  $Re = 1$ .

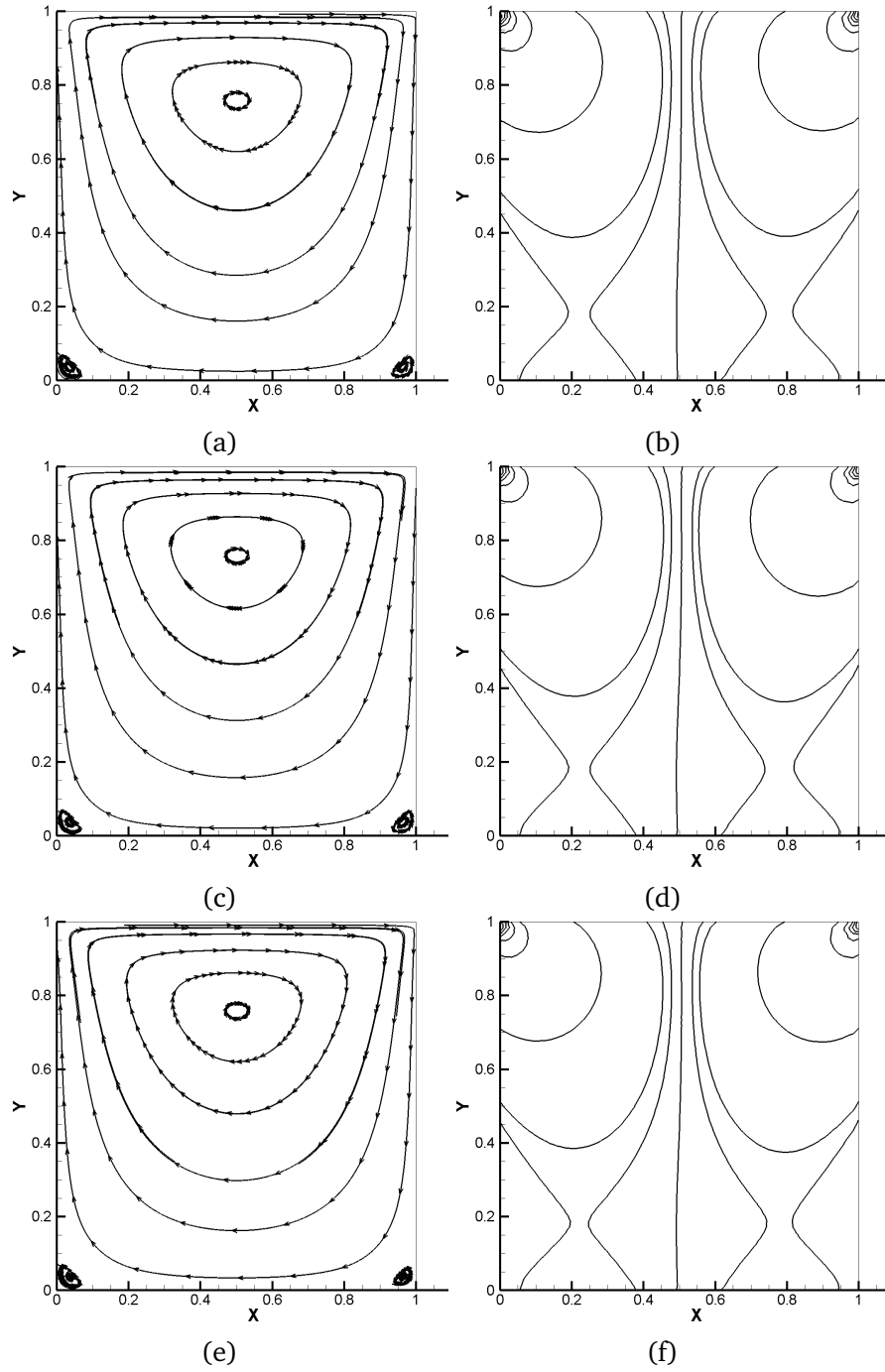


Figure 5: Velocity streamlines (a), (c), (e) and pressure level lines (b), (d), (f) by Algorithm II with  $\delta = 3.16, 0.316, 0.0316$  for  $Re = 1$ , respectively.

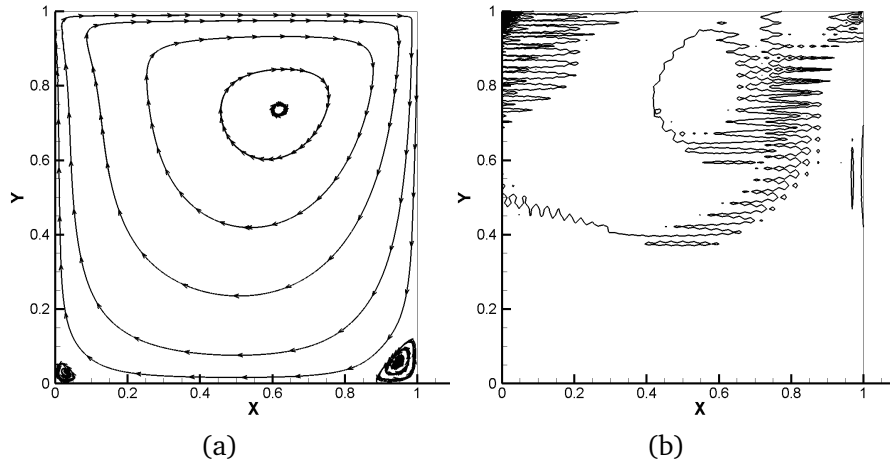


Figure 6: Velocity streamlines (a) and pressure level lines (b) by Algorithm II with  $\delta = 0.0316$  for  $Re = 100$ .

restrictive.

We also list the  $L^2$ -norm,  $H^1$ -norm of the velocity and  $L^2$ -norm of the pressure for the different values of  $Re$  in Table 4. The exact solution of this problem is unknown, so we cannot readily compute the error, but can compare the different norms of the actual finite element approximations obtained.

## 6. Conclusions

We have discussed three iterative stabilised FEMs for simulations obtained from the stationary Smagorinsky model. In general, the Newton iterative scheme performed best, reaching an optimal convergence rate with the small relative error and the least iterations for small Reynolds number ( $Re$ ) and filter radii ( $\delta$ ) values. However, none of the three iterative stabilised FEMs for the Smagorinsky model are suitable for large  $Re$  and  $\delta$  values, so a fast algorithm to deal with large Reynolds number should be sought. Future attention could also be given to other nonlinear or higher-dimensional problems.

## Acknowledgments

The authors thanks an editor and referees for their valuable comments and suggestions, which helped us to improve this article. The authors also thank Dr. Dongwei Gui (Cele National Station of Observation & Research for Desert-Grassland Ecosystem in Xinjiang) for his support and encouragement. The first author is partially supported by the Graduate Student Research Innovation Program of Xinjiang (No. XJGRI2013010) and the Excellent Doctor Innovation Program of Xinjiang University (No. XJUBSCX-2012015). The second author is partially supported by the NSF of Xinjiang Province (No. 2013211B01). The fourth author is partially supported by the Distinguished Young Scholars Fund of Xinjiang Province (No. 201311010) and the National Science Foundation of China (No. 11271313).

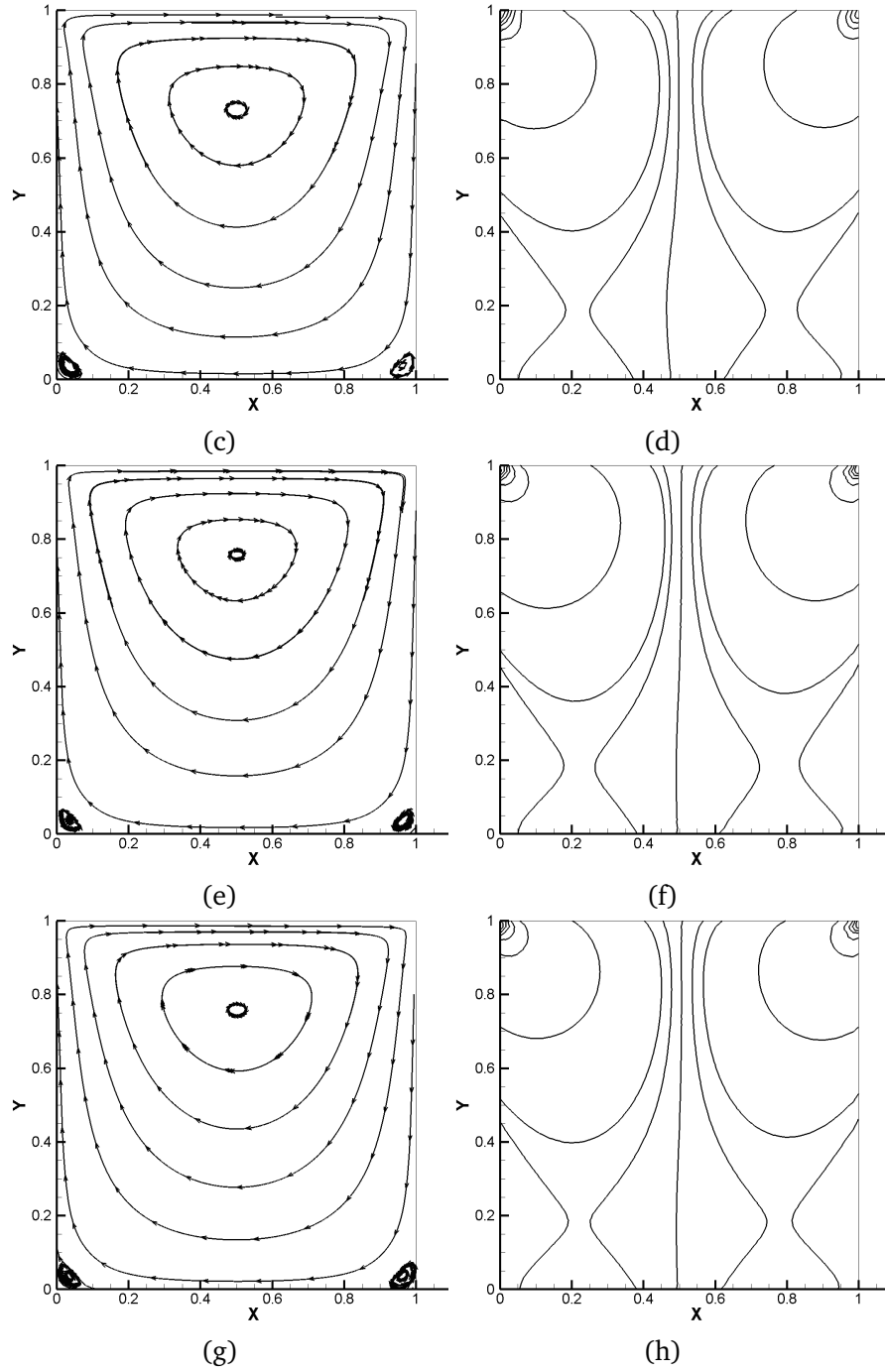


Figure 7: Velocity streamlines (a), (c), (e), (g) and pressure level lines (b), (d), (f), (h) by Algorithm III with  $\delta = 3.16, 0.316, 0.0316$  for  $Re = 1$ , respectively.



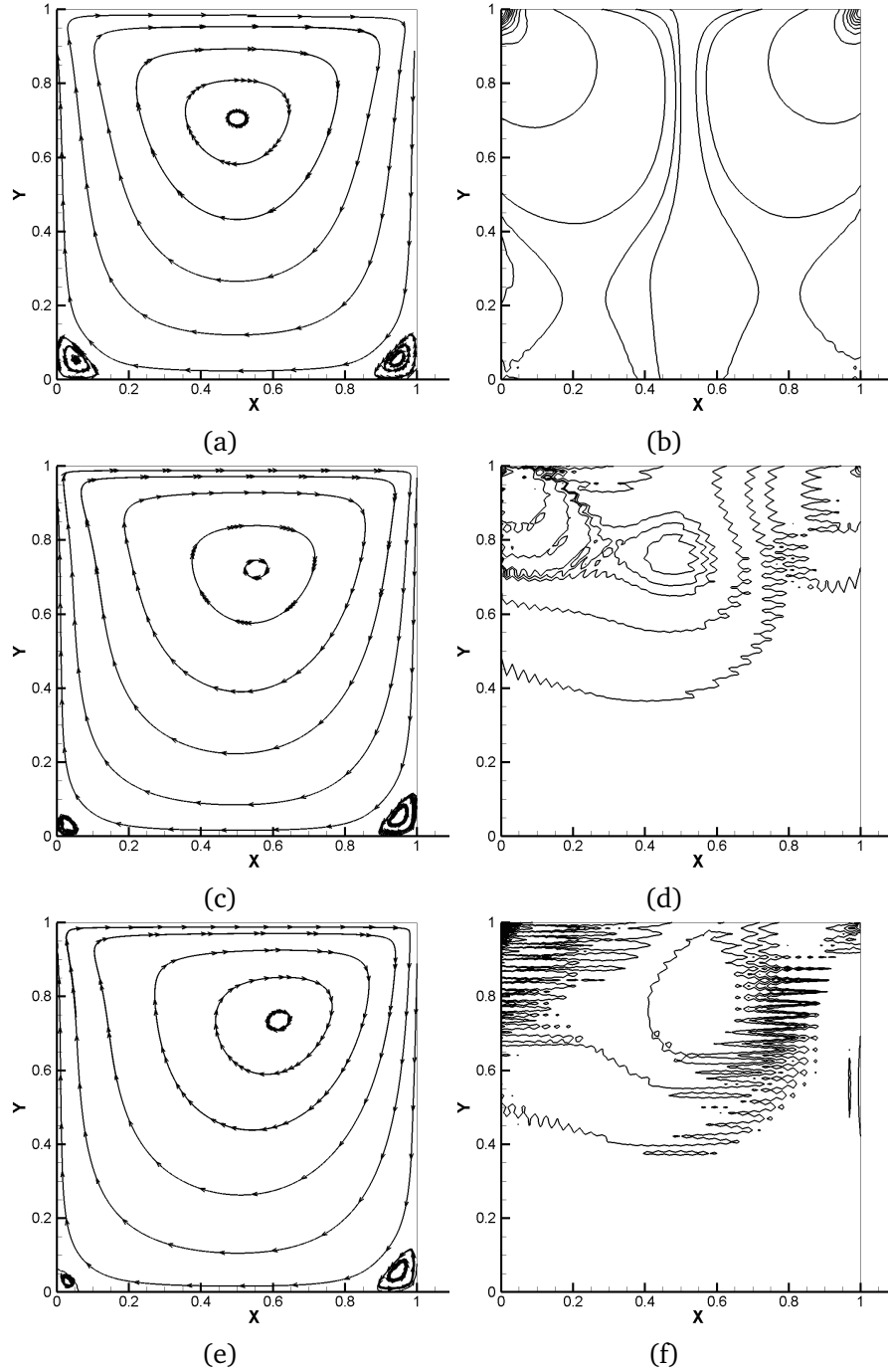


Figure 8: Velocity streamlines (a), (c), (e) and pressure level lines (b), (d), (f) by Algorithm III with  $\delta = 3.16, 0.316, 0.0316$  for  $Re = 100$ , respectively.

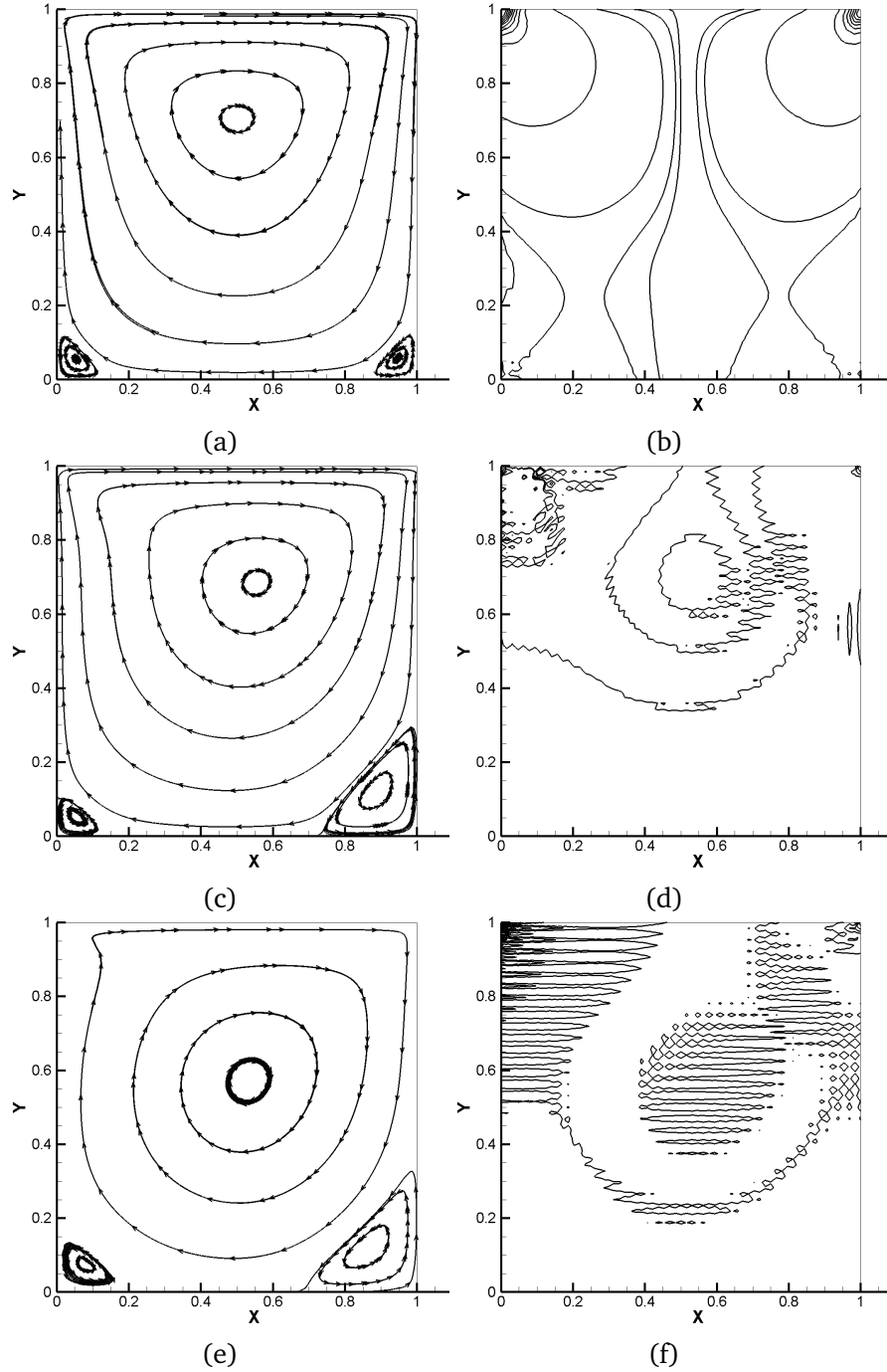


Figure 9: Velocity streamlines (a), (c), (e) and pressure level lines (b), (d), (f) by Algorithm III with  $\delta = 3.16, 0.316, 0.0316$  for  $Re = 1000$ , respectively.

Table 4: The  $H^1$ -relative-error,  $L^2$ -relative-error for  $u$  and  $L^2$ -relative-error for  $p$  for Algorithm I, II and III with various values of  $Re$  and  $\delta$  for the lid driven cavity.

Methods	$Re$	$\delta$	$u_{app}L^2 - error$	$u_{app}H^1 - error$	$p_{app}L^2 - error$
Algorithm I	1	31.6	N/A	N/A	N/A
Algorithm II	1	31.6	N/A	N/A	N/A
Algorithm III	1	31.6	0.267763	3.16825	535.510
Algorithm I	1	3.16	N/A	N/A	N/A
Algorithm II	1	3.16	0.219531	3.69437	6.58370
Algorithm III	1	3.16	0.242587	3.61852	24.0115
Algorithm I	1	0.316	N/A	N/A	N/A
Algorithm II	1	0.316	0.219509	3.69941	5.79773
Algorithm III	1	0.316	0.220322	3.69508	6.04363
Algorithm I	1	0.0316	0.218774	3.94219	6.41793
Algorithm II	1	0.0316	0.219508	3.69947	5.78972
Algorithm III	1	0.0316	0.219517	3.69942	5.79221
Algorithm I	100	3.16	N/A	N/A	N/A
Algorithm II	100	3.16	N/A	N/A	N/A
Algorithm III	100	3.16	0.255224	3.68660	19.6014
Algorithm I	100	0.316	N/A	N/A	N/A
Algorithm II	100	0.316	N/A	N/A	N/A
Algorithm III	100	0.316	0.241581	3.83705	0.456834
Algorithm I	100	0.0316	N/A	N/A	N/A
Algorithm II	100	0.0316	0.213076	3.94380	0.0987838
Algorithm III	100	0.0316	0.214274	3.93488	0.103159
Algorithm I	1000	3.16	N/A	N/A	N/A
Algorithm II	1000	3.16	N/A	N/A	N/A
Algorithm III	1000	3.16	0.255431	3.68783	19.5624
Algorithm I	1000	0.316	N/A	N/A	N/A
Algorithm II	1000	0.316	N/A	N/A	N/A
Algorithm III	1000	0.316	0.255453	3.91756	0.416410
Algorithm I	1000	0.0316	N/A	N/A	N/A
Algorithm II	1000	0.0316	N/A	N/A	N/A
Algorithm III	1000	0.0316	0.215617	4.77312	0.0500112

## References

- [1] R.A. Adams, J.J.F. Fournier, *Sobolev Spaces*. Academic Press, New York, 1975.
- [2] P.B. Bochev, C.R. Dohrmann & M.D. Gunzburger, *Stabilization of low-order mixed finite elements for the Stokes equations*, SIAM J. Numer. Anal. **44**, 82–101 (2006).
- [3] Y.N. He & J. Li, *Convergence of three iterative methods based on the finite element discretisation for the stationary Navier-Stokes equations*. Comput. Methods Appl. Mech. Engrg. **198**, 1351–1359 (2009).
- [4] X.L. Feng, I. Kim, H. Nam & D. Sheen, *Locally stabilized  $P_1$ -nonconforming quadrilateral and hexahedral finite element methods for the Stokes equations*, J. Comput. Appl. Math. **236**, 714–727 (2011).
- [5] P.Z. Huang, X.L. Feng & D.M. Liu, *Two-level stabilized method based on Newton iteration for*

- the steady Smagorinsky model*, Nonlinear Anal. Real World Appl. **14**, 1795–1805 (2013).
- [6] J. Borggaard & T. Iliescu, *Approximate deconvolution boundary conditions for large eddy simulation*, Appl. Math. Lett. **19**, 725–740 (2006).
  - [7] J. Borggaard, H. Lee, J.P. Roop & H. Son, *A two-level discretization method for the Smagorinsky model*, Multiscale Model. Simul. **7**, 599–621 (2008).
  - [8] J. Borggaard, T. Iliescu & J.P. Roop, *A bounded artificial viscosity large eddy simulation model*, SIAM, J. Numer. Anal. **47**, 622–645 (2009).
  - [9] J. Li & Z.X. Chen, *A new local stabilised nonconforming finite method for the Stokes equations*, Computing **82**, 157–170 (2008).
  - [10] J. Li & Y.N. He, *A new stabilised finite element method based on two local Gauss integrations for the Stokes equations*, J. Comput. Appl. Math. **214**, 58–65 (2008).
  - [11] L.C. Berselli, T. Iliescu & W.J. Layton, *Mathematics of Large Eddy Simulation of Turbulent Flows*, Scientific Computation. Springer-Verlag, Berlin, 2006.
  - [12] H.Y. Su, P.Z. Huang & X.L. Feng, *Two-level stabilized nonconforming finite element method for the Stokes equations*, Appl. Math. **58**, 643–656 (2013).
  - [13] T. Iliescu, & P.F. Fischer, *Large eddy simulation of turbulent channel flows by the rational LES model*, Phys. Fluids. **15**, 3036–3047 (2003).
  - [14] V. Girault & P.A. Raviart, *The Finite Element Method for Navier-Stokes Equations. Theory and Algorithms*. Springer-Verlag, Berlin, Heidelberg, 1986.
  - [15] X.X. Dai & X.L. Cheng, *A two-grid method based on Newton iteration for the Navier-Stokes equations* J. Comput. Appl. Math. **220**, 566–573 (2008).